IMPACT HEATING AND THE SOUTH POLAR THERMAL ANOMALY ON ENCELADUS. J. H. Roberts[1] and A. M. Stickle[1], [1]Johns Hopkins University Applied Physics Laboratory, 11100 Johns Hopkins Rd., Laurel, MD 20723, James.Roberts@jhuapl.edu

Introduction: Enceladus is well known for its south polar region [1]. The region is extremely young [2] and is characterized by four large, tidally-controlled fractures called the Tiger Stripes. Plumes of vapor and ice grains escape from the Tiger Stripes, along with several GW of heat, as measured by the Composite Infrared Spectrometer (CIRS) on Cassini [3]. Tidal dissipation is the probable source of this energy. However, models of the internal dynamics suggest that heat is removed from the interior faster than it can be produced, resulting in the geologically rapid freezing of any global subsurface ocean [4,5], although a regional sea may be longer-lived [6]. Tidal dissipation in the ice shell is severely restricted if it is mechanically coupled to the rigid silicate core. In such a scenario, if the ocean freezes entirely, tidal heating is predicted to drop precipitously. A further complication is that the heat flow and activity are observed only in the south polar region; no corresponding thermal anomaly is observed in the north. The tidal potential function is at spherical harmonic degree $\ell = 2$. This produces a pattern of tidal dissipation in the ice shell that is symmetric about the equator ($\ell = 2, 4$). This symmetry can be broken if there are significant lateral variations in the mechanical properties of the ice shell.

Here we examine the effects of a large impact on both the initial meltwater production, and on softening of the surrounding ice by the shock heating. We model the subsequent tidal dissipation and thermal evolution of the ice shell in response to the impact heating.

Impact of an impact: We use the CTH hydrocode [7] in axisymmetric geometry to simulate a vertical impact by an icy or rocky projectile into an ice shell. We treat the target as a half-space because the shock heating does not penetrate to the ocean unless the ice shell is implausibly thin. The target has a pressure-dependent yield surface, with a yield strength of 15 GPa [8]. We use the 5-phase ANEOS for ice [9] to compute the temperature change and melt production. In Figure 1, we show the temperature increase resulting from the impact of a 4 km diameter and a 15 km diameter icy projectile at 20 km/s, scaled to create a 150-km diameter crater (the approximate size of the south polar terrain [1]). We use a 1 km by 1 km tracer grid, and adaptive mesh refinement with a maximum resolution of 1.62 m. For the larger projectile, significant heating occurs up to 40 km deep and up to 30 km horizontally away from the impact.

Thermal Effects: We model thermal evolution in the ice shell using the finite-element code Citcom in 2D-axisymmetric geometry [10]. The viscosity is temperature-dependent [11]. The temperature is 75 K at the surface and 273 K at the base of the ice shell. We compute the tidal heating using the propagator-matrix code TiRADE [12] for a spherically symmetric body with an arbitrary number of visco-elastic layers [13].

We read in the impact heating and initial tidal heating into Citcom. Because the impact heating significantly reduces the viscosity locally, we perturb the tidal heating based on the local viscosity [12,14]. We allow the temperature to evolve for a short time, update the tidal heating based on the new temperature and viscosity structure in the ice shell and repeat for the duration of the model. In Figure 2, we show an example of the thermal evolution in a 40 km thick ice shell in response to the heating in Figure 1a, after the

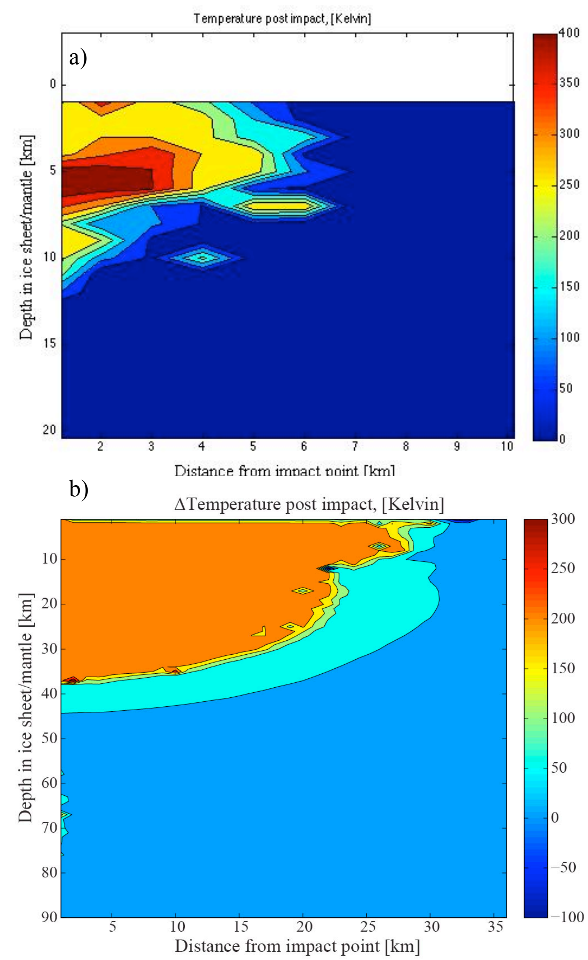

Figure 1: Impact-induced temperature increase resulting from impact of a 4-km diameter (top) and 15-km diameter (bottom) icy projectile into an icy halfspace at 20 km/s.

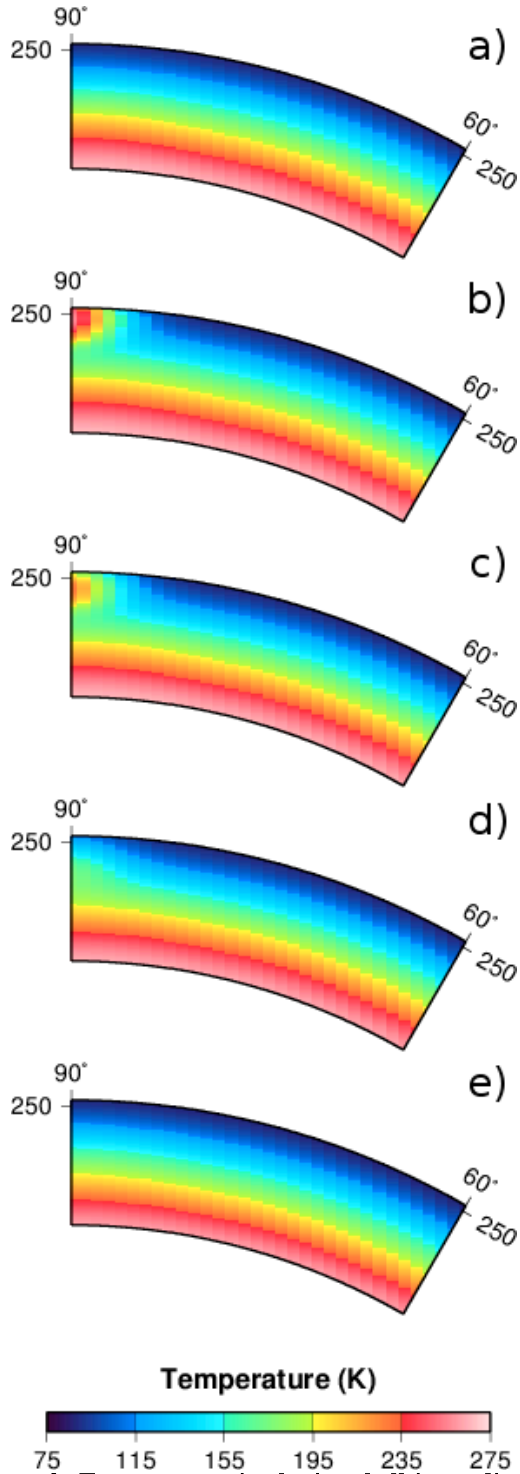

Figure 2: Temperature in the ice shell immediately before the impact (a), immediately after the impact (b), and after 0.1 My (c), 0.5 My (d), and 2 My (e).

heat consumed by melting is taken into account. In the case shown here, the ice shell is too thin to sustain convection; the impact is the sole significant source of lateral variation in temperature.

Discussion: The impact heating shown in Figures 1a and 2 is largely confined to the upper portion of the ice shell. Even in the absence of convection, this heating diffuses away in ~1 My. This result is broadly similar to that of earlier studies of a very slow collision with a co-orbital object [15]. Therefore, unless such an impact occurred in the very recent past, the thermal effects should not be observable today. The impact heating softens the ice and enhances the tidal heating locally. This enhancement is more self-sustaining. In the case shown, this is a relatively small effect, however the projectile studied is relatively small.

The impact shown in Figure 1 generates approximately 56500 km^3 of meltwater, down to about 37 km depth at the impact center. Melting of this thickness of ice corresponds to a reduction in elevation of ~3 km, and generating a substantial south polar sea. In the case where a pre-existing global ocean exists, the impact would melt a hole completely though any ice shell thinner than 37 km, enabling transfer of material between the surface and the ocean.

Larger impacts (e.g., Figure 1b), distribute their energy over a wider area and at greater depth. The impact-induced tidal enhancement should be correspondingly larger and longer-lived. Larger projectiles will also produce a greater degree of melting, and subsequent subsidence of the surface once the meltwater drains to the subsurface ocean. The resulting topography should be more consistent with the observed depression of the south polar terrain. The local thinning of the ice shell is also consistent with gravity measurements [16] that suggest a south polar sea [17] rather than a global ocean may be present.

References: [1] Thomas P. C. et al. (2007) *Icarus, 190*, 573-584. [2] Porco C. C. et al. (2006) *Science, 311*, 1393-1401. [3] Spencer J. R. et al. (2013) *DPS 45,* 403.03. [4] Roberts J. H. and Nimmo F. (2008) *Icarus, 194*, 675-689. [5] Tobie G. et al. (2008) *Icarus, 196*, 642-652. [6] Behounkova M. et al. (2011), *JGR, 115*, E09001. [7] McGlaun, J.M., et al. (1990), *Int. J. Impact Eng*., 10, 351-360. [8] Gold, L. W. (1977), *J. Glaciology, 19*, 197-212. [9] Senft L. E. and Stewart S. T. (2008), *MAPS, 43*, 1993-2013. [10] Roberts J. H. and Zhong S. (2004), *JGR, 109*, E06013. [11] Goldsby D. L. and Kohlstedt D. L. (2001) *JGR, 106*, 11017-11030. [12] Roberts J. H. (2013) *LPSC, 44,* 1317. [13] Sabadini R. and Vermeersen B. (2004) *Applications of Normal Mode Relaxation Theory to Solid-Earth Geophysics*, Kluwer Acad. Pub. [14] Sotin C. et al., (2002) *GRL, 29*, 74-1-74-4. [15] Peale S. J. and Greenberg R. (2007) *AGU Fall Meet. 2007*, P12B-02. [16] Iess L. et al. (2014) *Science, 344*, 78-80. [17] Collins G. C. and Goodman J. C., *Icarus, 189*, 72–82.